ACS APPLIED MATERIALS & INTERFACES

Research Article

www.acsami.org

Electrochemical Performance of Porous Diamond-like Carbon Electrodes for Sensing Hormones, Neurotransmitters, and Endocrine Disruptors

Tiago A. Silva,[†] Hudson Zanin,*[,‡] Paul. W. May,[‡] Evaldo J. Corat,[§] and Orlando Fatibello-Filho[†]

[†]Department of Chemistry, Federal University of São Carlos, Rodovia Washington Luís km 235, 676, São Carlos, 13560-970, SP Brazil

[‡]School of Chemistry, University of Bristol, Cantocks Close, Bristol BS8 1TS, United Kingdom

[§]National Institute for Space Research, Avenida dos Astronautas 1758, Sao Jose dos Campos, 12227-010, SP Brazil

ABSTRACT: Porous diamond-like carbon (DLC) electrodes have been prepared, and their electrochemical performance was explored. For electrode preparation, a thin DLC film was deposited onto a densely packed forest of highly porous, vertically aligned multiwalled carbon nanotubes (VACNT). DLC deposition caused the tips of the carbon nanotubes to clump together to form a microstructured surface with an enlarged surface area. DLC:VACNT electrodes show fast charge transfer, which is promising for several electrochemical applications, including electroanalysis. DLC:VACNT electrodes were applied to the determination of targeted molecules such as dopamine (DA) and epinephrine (EP), which are neurotransmitters/hormones, and acetaminophen (AC), an endocrine disruptor. Using simple and low-cost techniques, such as cyclic voltammetry, analytical curves in the concentration range from 10 to 100 μmol L^{-1} were obtained and excellent analytical parameters achieved, including high analytical sensitivity, good response stability, and low limits of detection of 2.9, 4.5, and 2.3 μmol L^{-1} for DA, EP, and AC, respectively.

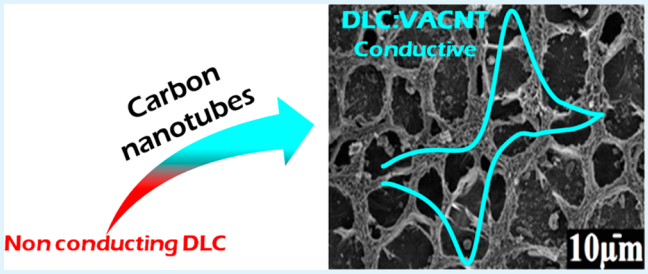

KEYWORDS: *porous DLC, fast charge transfer, aligned nanotubes scaffold, electroanalysis*

1. INTRODUCTION

Carbon is a very attractive material for electrochemical applications, due to its different allotropes (fullerenes, nanotubes, graphene, and diamond) of dimensionality from 0D to 3D.[1] Carbon materials can be prepared in various microtextures from powders to freestanding fibers, foams, amorphous materials, crystals, and composites.[2,3] By applying them as electrodes, they have shown reversibility properties in redox processes, with fast charge transfer and chemical stability in strongly acidic or basic solutions with good performance over a wide range of potential and temperature.[4−6] The rate of electron transfer at carbon electrodes depends on various factors, such as the structure, morphology, and conductivity of the material.[7] All those characteristics are directly related to the carbon hybridization.

Diamond-like carbon (DLC) is an interesting metastable form of amorphous carbon[8] that contains a mixture of tetrahedral (sp^3) and trigonal (sp^2) carbon hybridizations in varying amounts depending on its deposition conditions. Although DLC can be deposited at low (<200 °C) substrate temperature,[9,10] it exhibits many of the extreme properties of crystalline diamond.[11] Among those properties are chemical inertness, optical transparency, high mechanical hardness, low friction coefficient, and very high electrical resistance, which together make DLC very attractive for use as a protective coating.[12−14] However, unmodified DLC films are electrically insulating, which prevents their application in several fields, including electroanalysis. To overcome this problem, there have been many attempts to improve the electrical conductivity of DLC by adding n- and p-type dopants.[15−19] Nevertheless, rather than dope the DLC with another element, a better option might be to incorporate conducting forms of carbon, such as carbon nanotubes (CNTs), into the DLC. Being cylindrical forms of graphene, CNTs are highly conductive and could improve the conductivity of diamond-like material by providing conductive pathways throughout the structure[20,21] and potentially overlapping the valence and the conduction bands of DLC. Nevertheless, only a few papers[22−26] report attempts to combine multiwalled (MW) CNTs and DLC to create an all-carbon electrode. Also all of those reports mainly concentrate on the effect of CNTs incorporation on the DLC's mechanical properties.

Recently we reported two different methods to incorporate MWCNT into DLC.[26,27] We first reported incorporation of MWCNT powder into the bulk of a DLC film and its effect on the film's mechanical, structural, optical, and electrochemical

Received: September 2, 2014
Accepted: November 17, 2014
Published: November 17, 2014

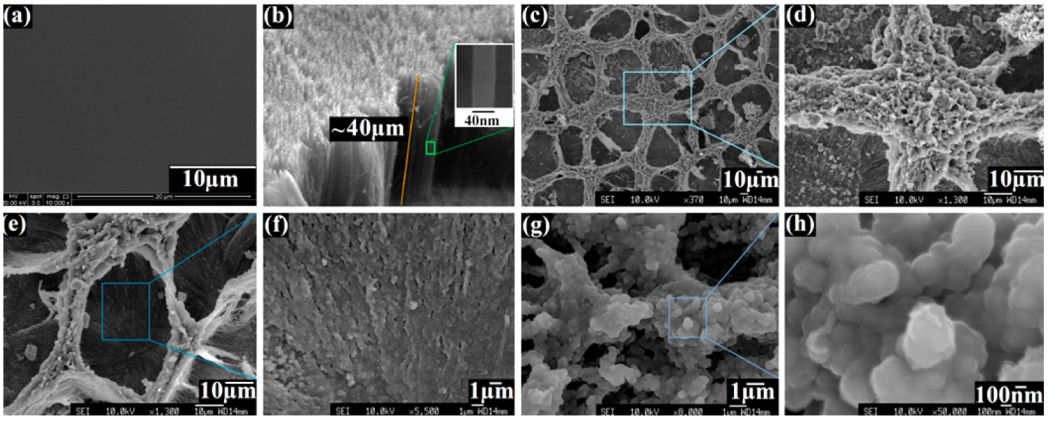

Figure 1. SEM images of the sample morphologies: (a) the DLC:Si film; (b) the as-grown VACNT scaffold, with an inset showing a very high magnification image of a single CNT; (c, e, and g) top views of the DLC:VACNT composite showing the honeycomb structures; and higher magnification images of the (d and h) crests and (f) valleys.

properties. We concluded that, by percolation, the MWCNTs create conductive pathways that transport current rapidly to all parts of the film, including the surface regions, where they can contribute to electrochemical redox reactions.[27] In a second paper, we presented a method to prepare high surface area DLC electrodes, which show excellent field emission properties, using a forest of vertically aligned multiwalled carbon nanotubes (VACNTs) as scaffolds[26] for DLC deposition. DLC deposition caused the tips of the CNTs to clump together to form a microstructured surface with a very large surface area. Different microstructures, such as pointed "teepees", elongated ridges, or "honeycombs" could be fabricated, depending on the areal density of the VACNTs. Such high surface area, chemically stable, conducting structures appear to be an ideal material for use as electrodes for electroanalytical determination of organic and inorganic compounds in aqueous media.

The aim of this work is to evaluate these porous DLC electrodes for electroanalytical determination of important hormones, neurotransmitters, and endocrine disruptors using simple, fast, and low-cost cyclic voltammetry techniques.

2. EXPERIMENTAL SECTION

To prepare the porous DLC electrodes, thin DLC films were deposited onto densely packed forests of VACNT electrodes, as described below.

2.1. Synthesis of VACNT Films. The VACNT films were produced using a microwave-plasma (MWCVD) chamber operating at 2.45 GHz.[28] Prior deposition, Ti substrates (10 mm × 10 mm × 0.5 mm) were covered with a 10 nm Ni layer deposited by electron-beam evaporation. The Ni layer was heated in a N_2/H_2 (10/90 sccm) plasma, which caused it to ball up into nanoclusters that subsequently became the catalyst particles for VACNT growth. The nanocluster formation took place as the substrate temperature increased from 350 to 800 °C over a period of 5 min. To grow the VACNT forest, CH_4 (14 sccm) was introduced into the chamber for 1 min, a substrate temperature of 800 °C being maintained. The reactor pressure was 30 Torr during all procedures. This process produces a high spatial density of aligned CNTs ~40 μm long and ~40−50 nm thick.[28]

2.2. Synthesis of DLC Films. The DLC layers were deposited using a plasma-enhanced CVD (PECVD) reactor fed with hexane vapor and argon gas at 0.1−0.3 Torr and a discharge voltage of −700 V at a pulse frequency of 20 kHz. For porous DLC preparation, the previously prepared VACNT forest was used as a substrate. Before growth, *n*-hexane was sprayed onto the samples, causing the tips of the CNTs to stick together due to liquid surface tension. Then the plasma was struck under argon and *n*-hexane vapor for 10 min,[26] depositing DLC onto the microstructured surface, locking the structure into place. This DLC-coated VACNT electrode has been named as DLC:VACNT electrode.

In contrast, flat DLC electrodes were deposited onto a polished silicon substrate for use as control samples (called as DLC:Si electrode). To prepare these, a single-crystal Si(100) wafer was placed into the PECVD reactor and cleaned using an argon plasma atmosphere at 0.1 Torr (Ar flow rate of 1 sccm) for 30 min. Next, *n*-hexane was sprayed into the active plasma region via a nozzle directed downward onto the substrate surface for 1 h to deposit 1 μm of DLC, with Ar flowing during the whole process. After deposition, the samples were cooled down in high vacuum (10^{-6} Torr) for 3 h.[27]

2.3. Materials Characterization. The samples were characterized by high-resolution scanning electron microscopy (HR-SEM), Raman spectroscopy, and electrochemical tests. HR-SEM was performed with a JEOL6330 and FEI Inspect F50 operated at 10−20 kV. Raman spectra were recorded at room temperature using a Renishaw microprobe, employing argon ion laser excitation (λ = 514.5 nm) with a laser power of ~6 mW and a spot size ~15 μm. Curve fitting and data analysis Fityk software was used to assign the peak locations and fit all spectra.

2.4. Electrochemical Assays. The electrochemical assays were conducted in a conventional three-electrode cell, using an Ag/AgCl (3.0 mol L^{-1} KCl) reference electrode, a Pt foil as counter electrode, and the DLC:VACNT electrode as the working electrode. The working electrode was encapsulated by a copper/Teflon electrochemical cell, which includes an electrical contact to a copper rod on the back-side of the sample and exposes a fixed area of electrode (0.44 cm^2) exposed to the solution. A potentiostat/galvanostat μAutolab type III (Ecochemie) controlled with GPES software (version 4.9) was employed for the electrochemical measurements.

The electrochemical sensing performance of the DLC:VACNT electrode was assessed for the important biomolecules dopamine (DA), epinephrine (EP), and acetaminophen (AC) by cyclic voltammetry (CV). In this evaluation, the electrochemical behavior of the compounds was explored, and their analytical parameters were determined from analysis of the respective analytical curves. All the CV experiments for DA, EP, and AC were conducted in 0.2 mol L^{-1} phosphate buffer solution at pH 7.0. CVs were collected with the analyte concentration ranging from 10 to 100 μmol L^{-1} recorded from 10 to 400 mV s^{-1}. All chemicals were purchased from Sigma-Aldrich.

3. RESULTS AND DISCUSSION

3.1. Material Characterization. SEM images of the DLC:VACNT composite contrasted with those of VACNT and DLC:Si films are shown in Figure 1a−h. The typical morphology of the DLC control sample is presented in Figure 1a, revealing a flat, featureless film. Used as a scaffold for porous

DLC deposition, the as-grown VACNT forest is shown in Figure 1b and highlights its alignment, high spatial density, and relatively flat, carpetlike surface. The CNTs are ~40 μm long and about 40−50 nm thick (inset in Figure 1 b).

The top view of the DLC:VACNT film shows a microstructure (Figure 1c,e) indicating that after a few minutes of DLC deposition the VACNT tips have stuck together. The DLC coating has caused the CNTs to form linked rings. The type of microstructuring (teepees, honeycombs, two-dimensional ridges, or spiderwebs) seen when depositing films onto CNTs depends mostly upon the density and length of CNT growth,[26] and for these VACNTs, the density was such that honeycomb structures predominate.

High-resolution images from regions of the microstructure reveal details of the valleys and peaks of the honeycombs (Figure 1d,f−h). On the crests of the honeycomb edges one can see a buildup of DLC, as shown in Figure 1d,g,h. It appears that some of the crests (Figure 1d) are formed by thousands of nanotubes encapsulated together by the DLC film. Other crests are formed by 50−100 nanotubes, as shown in Figure 1g,h. In the valleys (Figure 1f), it is observed that the nanotubes maintain alignment even after being covered by DLC.

Figure 2 shows typical Raman spectra of the DLC:VACNT composite, DLC:Si, and the as-grown VACNT forest. The

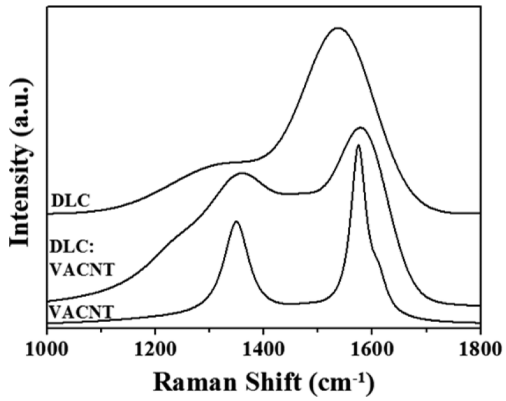

Figure 2. Raman spectra of the DLC:VACNT, DLC:Si, and VACNT materials.

DLC spectrum is typical of that seen from amorphous carbon films, showing two broad Gaussian bands, the D-band centered at 1340 cm^{-1}, resulting from the breathing mode of sp^2 carbon sites in rings but not chains, and the G-band centered at ~1537 cm^{-1}, arising from stretching of any pair of sp^2 sites whether in rings or chains.[29,30] The VACNT first-order Raman spectrum has two pronounced peaks centered at 1357 cm^{-1} (D-band) and 1585 cm^{-1} (G-band). In the case of graphite or graphitic CNTs, the D-band is related to defects and disordered carbon, while the G-band (E_{2g}) is related to well-ordered crystalline graphite.[31] The D′-peak (1622 cm^{-1}) is also observed and is also correlated to disorder. The VACNT second-order Raman spectrum (data not shown) revealed a pronounced G′-peak, confirming the good crystallinity of VACNT.

The Raman spectrum of the DLC:VACNT composite is a combination of both DLC and VACNT Raman characteristics. Clearly, for DLC:VACNT the narrower VACNT D-band appears combined with the broader DLC one, and the G-band shows a broader feature involving the DLC G-band and the VACNT G- and D′-bands. This indicates that the DLC has not replaced the CNTs but simply coated them.

3.2. Electrochemical Response of DA, EP, and AC Molecules on the DLC:VACNT. The influence of the CNT incorporation on the electrochemical behavior of the DLC film was then explored for sensing of selected hormones, neurotransmitters, and endocrine disruptors. In this study we have chosen molecules with well-known electrochemical responses, such as the neurotransmitters/hormones DA and EP, and the endocrine disruptor AC,[32,33] allowing us to compare the sensitivity of this new electrode with standard alternatives.

CV experiments were conducted over a large scan-rate range in order to investigate the electron-transfer process of the selected molecules on the DLC:VACNT electrode. All the CV experiments for DA, EP, and AC were conducted in 0.2 mol L^{-1} phosphate buffer solution at pH 7.0.

The CVs recorded from 10 to 400 mV s^{-1} performed for all three molecules are shown in Figure 3a−c. DA and AC show quasi-reversible characteristics, while EP shows an irreversible profile. The evaluation of the peak currents (I_p) as a function of the square root of the scan rate (ν) revealed a linear relationship (see insets in Figure 3a−c), indicating that the electrodic processes were governed only by diffusion.[34−36] Furthermore, as expected for the case of semi-infinite linear diffusion (Randles−Ševćik equation),[34] plots of log I_p versus log ν were linear with slopes of 0.57 (DA), 0.39 (EP), and 0.50 (AC). These are all close to the expected theoretical value of 0.5 for a diffusion-controlled process.[34,35,37]

Assuming that the analytes on the DLC:VACNT electrode were controlled by their diffusional mass transport, we have selected the appropriated theories to determine the respective values of the kinetic parameter heterogeneous electron-transfer rate constant (k^0). DA and AC showed quasi-reversible behavior, and therefore, the Nicholson method[38] for quasi-reversible diffusion-controlled processes was selected for these compounds. For EP, the approach proposed by Nicholson and Shain[39] was employed, which is applicable to irreversible diffusion-controlled processes.

The Nicholson method establishes a relation between the kinetic parameter Ψ and the inverse of the square root of the scan rate ($\nu^{-1/2}$) with k^0 as the proportionality term, as shown in eq 1

$$\Psi = k^0[\pi D n \nu F/(RT)]^{-1/2} \quad (1)$$

where D is the diffusion coefficient and the other terms have their usual meanings. Thus, k^0 can be predicted from the gradient of a Ψ vs $\nu^{-1/2}$ plot. To obtain the Ψ values, we used eqs 2 and 3 proposed by Lavagnini et al.,[40] which relate Ψ and the ΔE_p (peak-to-peak potential separation) value for each scan rate

$$\Psi = (-0.6288 + 0.0021 n\Delta E_p)/(1 - 0.017 n\Delta E_p) \quad (2)$$

$$\Psi = 2.18(\beta/\pi)^{1/2} \exp[-(\beta^2 F/RT) n\Delta E_p] \quad (3)$$

where β is the transfer coefficient in eq 3 and the other terms have their usual meanings. Equation 2 is employed for those cases in which $n\Delta E_p$ < 200 mV, while eq 3 is used when $n\Delta E_p$ > 200 mV. The values of $n\Delta E_p$ range from 84 to 434 mV for DA and from 114 to 600 mV for AC, assuming that two electrons are involved in the electrooxidation of the two molecules.[41,42] Therefore, each equation (eq 2 or 3) was used for Ψ calculation in its respective $n\Delta E_p$ range of validity. From the calculated Ψ values, the k^0 parameter follows from the gradient of the Ψ vs $23.66\nu^{-1/2}$ plot for DA and Ψ vs $10.37\nu^{-1/2}$ plot for AC. The

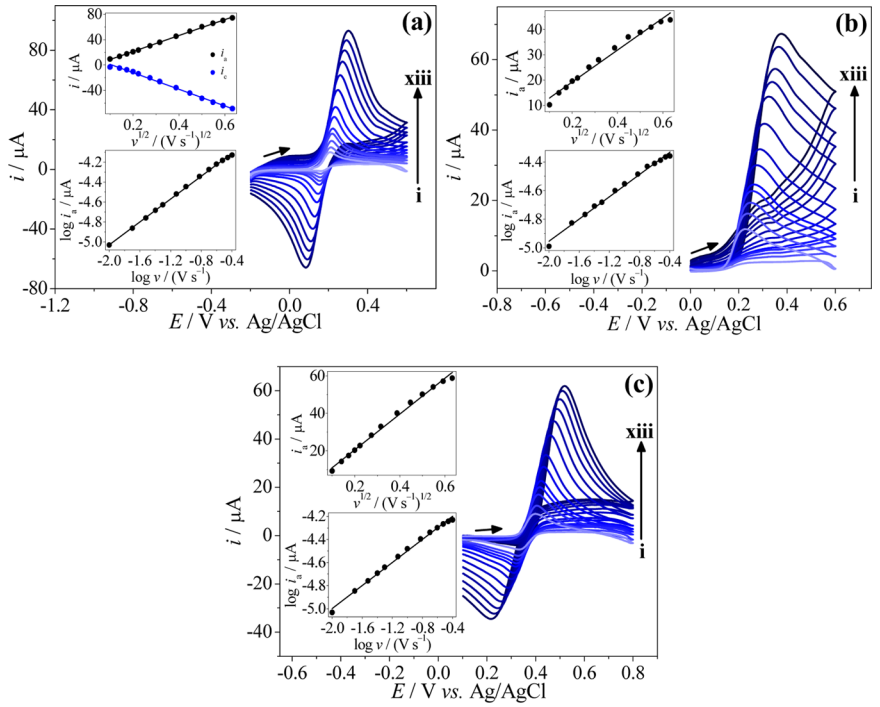

Figure 3. CVs obtained for (a) 1.0×10^{-4} mol L^{-1} DA, (b) 1.0×10^{-4} mol L^{-1} EP, and (c) 1.0×10^{-4} mol L^{-1} AC in 0.2 mol L^{-1} phosphate buffer solution (pH 7.0) using the DLC:VACNT electrode at different scan rates (ν): (i) 10 mV s^{-1}, (ii) 20 mV s^{-1}, (iii) 30 mV s^{-1}, (iv) 40 mV s^{-1}, (v) 50 mV s^{-1}, (vi) 75 mV s^{-1}, (vii) 100 mV s^{-1}, (viii) 150 mV s^{-1}, (ix) 200 mV s^{-1}, (x) 250 mV s^{-1}, (xi) 300 mV s^{-1}, (xii) 350 mV s^{-1}, and (xiii) 400 mV s^{-1}. Insets: i_a vs $\nu^{1/2}$ and log i_a vs log ν curves.

23.66 and 10.37 factors are equivalent to the term $[\pi DnF/(RT)]^{-1/2}$ in eq 1, calculated considering D(DA) = 7.3×10^{-6} cm^2 s^{-1},[42] D(AC) = 3.8×10^{-5} cm^2 s^{-1},[43] F = 96 485 C mol^{-1}, R = 8.314 J K^{-1} mol^{-1}, and T = 298.15 K. A linear best fit gives $k^0 = 5.2 \times 10^{-3}$ cm s^{-1} for DA and 4.5×10^{-3} cm s^{-1} for AC. The results indicate a similar electron-transfer rate for both DA and AC on the DLC:VACNT electrode. Moreover, the electron-transfer rate constants were similar to typical results found by other workers for DA and AC using a modified CNT paste electrode (DA, 2.21×10^{-3} cm s^{-1})[42] and a bare graphite electrode (AC, 4.8×10^{-3} cm s^{-1}).[44]

For k^0 determination of EP, Nicholson and Shain's method was employed. According to this method, the peak current has an exponential relationship with the difference between the peak potential (E_p) and the formal potential ($E°$) in diffusional irreversible redox processes, eq 4

$$I_p = 0.227nFACk^0 \exp\left[\left(\frac{\alpha nF}{RT}\right)(E_p - E°)\right] \quad (4)$$

where C is the electroactive species concentration ([EP] = 1.0×10^{-7} mol cm^{-3}), A is the geometric area of the working electrode (0.44 cm^2 in this work), and the other terms have their usual meanings and values. Rearranging eq 4 gives

$$\ln I_p = \ln(0.227nFACk^0) + \left(\frac{\alpha nF}{RT}\right)(E_p - E°) \quad (5)$$

From eq 5, k^0 can be determined from the gradient of an ln I_p vs $(E_p - E°)$ linear plot. The value of $E°$ was determined at each current calculated[45] as $I = 0.82I_p$ for the different scan rates, and the average value found in this experiment was $E°$ = 0.25 ± 0.04 V. Therefore, k^0 was calculated by comparing the gradient of the ln I_p vs $(E_p - E°)$ curve with the gradient given by the Nicholson–Shain equation[39] (eq 5) assuming that two electrons are transferred in the EP electrooxidation.[46] A k^0 value of 8.9×10^{-3} cm s^{-1} was obtained. As observed for DA and AC, the k^0 value determined for EP was higher than the values reported on various other electrode materials, including glassy carbon electrodes modified with CNTs and ionic liquid (1.17×10^{-3} cm s^{-1}),[47] carbon paste electrode (CPE, 1.47×10^{-3} cm s^{-1}),[46] CPE modified with CNTs (2.13×10^{-3} cm s^{-1}),[46] CPE modified with sodium dodecyl sulfate (SDS) (4.51×10^{-3} cm s^{-1}),[46] and CPE modified with CNTs and SDS (6.38×10^{-3} cm s^{-1}).[46] This electrokinetic study shows that incorporation of CNTs improve the charge transfer of DLC.

In addition to the previous exploration of the electrochemical behavior of the DA, EP, and AC molecules, we assessed the electroanalytical potentialities of the DLC:VACNT electrode for sensing of these target analytes. Thus, analytical curves for the three compounds were constructed using CV. CVs were collected with the analyte concentration ranging from 10 to 100 μmol L^{-1}, as shown in Figure 4a–c. In this concentration range, analytical curves with excellent correlation coefficients were obtained for all molecules (Figure 4d–f). Table 1 contains the parameters recorded from the analytical curves. In Table 1 the limit of detection (LOD) values were estimated using eq 6:

$$\text{LOD} = 3\sigma/m \quad (6)$$

where σ is the standard deviation of 10 blank (electrolyte only) measurements and m is the gradient of the analytical curve. A high analytical sensitivity was observed for the sensing of the molecules investigated, with signal variation 0.2–0.3 μA $\mu$$mol^{-1}$ L. The linear range and LODs calculated are excellent when compared to those reported for different electrode materials using CV to detect DA,[48−51] EP,[52,53] and AC.[41,54−56] The stability of response of the proposed electrode material was also evaluated from a study of repeatability, in which various CV measurements were performed for solutions of both analytes at

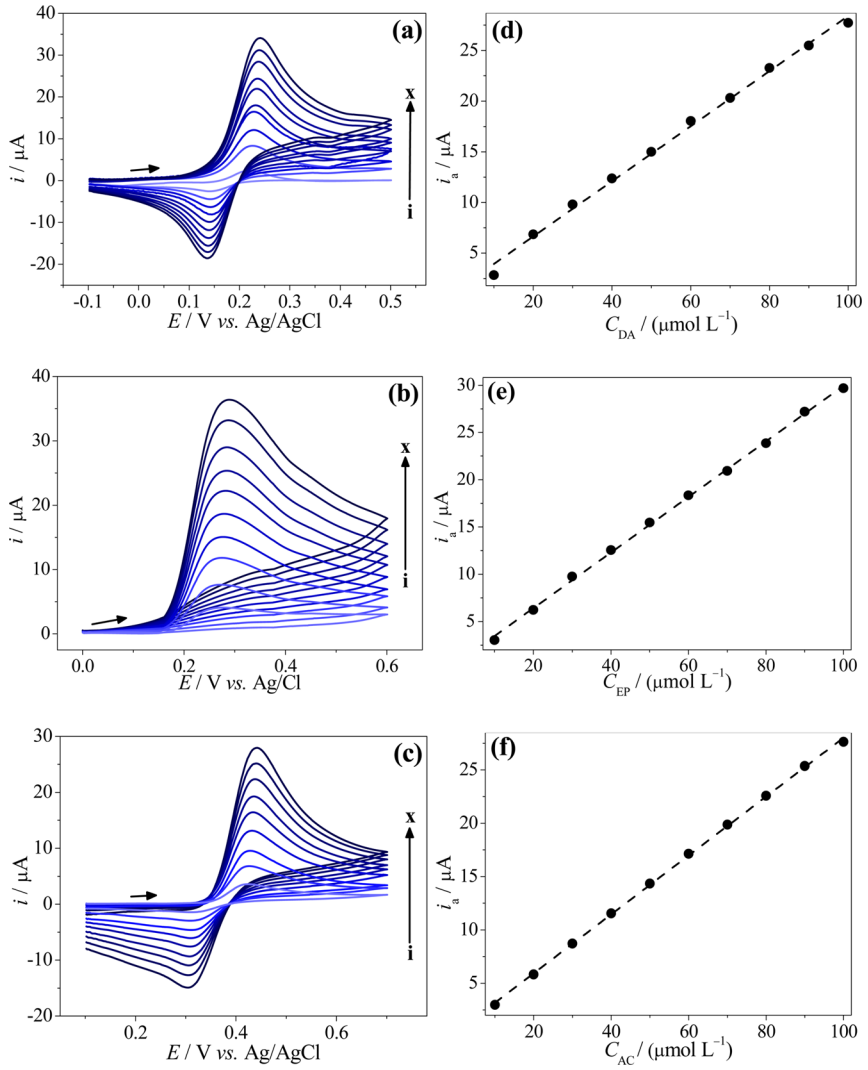

Figure 4. CVs obtained for (a) DA, (b) EP, and (c) AC at different concentrations: (i) 10 μmol L^{-1}, (ii) 20 μmol L^{-1}, (iii) 30 μmol L^{-1}, (iv) 40 μmol L^{-1}, (v) 50 μmol L^{-1}, (vi) 60 μmol L^{-1}, (vii) 70 μmol L^{-1}, (viii) 80 μmol L^{-1}, (ix) 90 μmol L^{-1}, and (x) 100 μmol L^{-1} in 0.2 mol L^{-1} phosphate buffer solution (pH 7.0) using the DLC:VACNT electrode. ν = 100 mV s^{-1}. Analytical curves constructed for (d) DA, (e) EP, and (f) AC.

Table 1. Analytical Parameters Obtained for Cyclic Voltammetric Determination of DA, EP, and AC Using the DLC:VACNT Electrode

analyte	sensitivity (μA μmol^{-1} L)	linear range (μmol L^{-1})	LOD (μmol L^{-1})
DA	0.27	10–100	3.9
EP	0.29	10–100	4.5
AC	0.28	10–100	2.3

Table 2. Relative Standard Deviations (RSD) Obtained for the Anodic Peak Current Registered during 10 Voltammetric Cycles (n = 10) for DA, EP, and AC Solutions at Different Concentration Levels Using the DLC:VACNT Electrode

analyte	concn (μmol L^{-1})	RSD (%)
DA	30.0	2.9
	50.0	3.5
EP	30.0	1.6
	50.0	1.9
AC	30.0	6.7
	50.0	3.1

different concentration levels. The results of relative standard deviations (RSD) obtained for the variation of the peak current during 10 successive CV determinations of DA, EP, and AC solutions at two concentration levels (30.0 and 50.0 μmol L^{-1}) are shown in Table 2. Low RSDs values ranging from 1.6 to 6.7% were observed, indicating the good precision of measurement of the DLC:VACNT electrode. The results demonstrate the electroanalytical potential of the novel DLC:VACNT electrode for determination of important target analytes. Other investigations into the use of these DLC:VACNT electrodes as electrochemical sensors to detect organic and inorganic compounds in different sample matrices are underway in our laboratories.

4. CONCLUSIONS

Porous diamond-like carbon electrodes fabricated by depositing DLC onto vertically aligned CNTs were applied for electroanalytical determination of hormones, neurotransmitters, and endocrine disruptors, including dopamine, epinephrine, and acetaminophen. These porous DLC:VACNT electrodes exhibit fast electron transfer and have high surface area, which are highly sensitive for analysis and present low limits of detection

of 2.9, 4.5, and 2.3 μmol L^{-1} for these three analytes, respectively.

AUTHOR INFORMATION

Corresponding Author

*E-mail: hudsonzanin@gmail.com.br . Tel: +44 (0) 117 462529137.

Notes

The authors declare no competing financial interest.

ACKNOWLEDGMENTS

We gratefully acknowledge the Electron Microscopy Unit of the School of Chemistry at University of Bristol and LME/LNLS-Campinas for microscopy support. The authors also want to thanks the Brazilian agency CNPq (202439/2012-7) for financial support.

REFERENCES

(1) Frackowiak, E.; Béguin, F. Carbon Materials for the Electrochemical Storage of Energy in Capacitors. *Carbon* **2001**, *39* (6), 937−950.

(2) Terrones, M. Science and Technology of the Twenty-First Century: Synthesis, Properties, and Applications of Carbon Nanotubes. *Annu. Rev. Mater. Res.* **2003**, *33* (1), 419−501.

(3) Umemoto, K.; Saito, S.; Berber, S.; Tománek, D. Carbon Foam: Spanning the Phase Space between Graphite and Diamond. *Phys. Rev. B: Condens. Matter Mater. Phys.* **2001**, *64* (19), 193409 (1)−193409 (3).

(4) Zanin, H.; Saito, E.; Ceragioli, H. J.; Baranauskas, V.; Corat, E. J. Reduced Graphene Oxide and Vertically Aligned Carbon Nanotubes Superhydrophilic Films for Supercapacitors Devices. *Mater. Res. Bull.* **2014**, *49*, 487−493.

(5) Borges, R. S.; Reddy, A. L. M.; Rodrigues, M.-T. F.; Gullapalli, H.; Balakrishnan, K.; Silva, G. G.; Ajayan, P. M. Supercapacitor Operating at 200 Degrees Celsius. *Sci. Rep.* **2013**, *3*, 2572(1)−2572(6).

(6) Chen, P.; McCreery, R. L. Control of Electron Transfer Kinetics at Glassy Carbon Electrodes by Specific Surface Modification. *Anal. Chem.* **1996**, *68* (22), 3958−3965.

(7) Nugent, J. M.; Santhanam, K. S. V.; Rubio, A.; Ajayan, P. M. Fast Electron Transfer Kinetics on Multiwalled Carbon Nanotube Microbundle Electrodes. *Nano Lett.* **2001**, *1* (2), 87−91.

(8) Robertson, J. Diamond-Like Amorphous Carbon. *Mater. Sci. Eng., R* **2002**, *37* (4−6), 129−281.

(9) Bewilogua, K.; Cooper, C. V.; Specht, C.; Schröder, J.; Wittorf, R.; Grischke, M. Effect of Target Material on Deposition and Properties of Metal-Containing DLC (Me-DLC) Coatings. *Surf. Coat. Technol.* **2000**, *127* (2−3), 223−231.

(10) Costa, R. P. D. C.; Marcian, F. R.; Oliveira, D. A. L.; Trava-Airoldi, V. J. Enhanced DLC Wear Performance by the Presence of Lubricant Additives. *Mater. Res.* **2011**, *14*, 222−226.

(11) Zeng, A.; Neto, V. F.; Gracio, J. J.; Fan, Q. H. Diamond-Like Carbon (DLC) Films as Electrochemical Electrodes. *Diamond Relat. Mater.* **2014**, *43*, 12−22.

(12) Omer, A. M. M.; Adhikari, S.; Adhikary, S.; Rusop, M.; Uchida, H.; Soga, T.; Umeno, M. Electrical Conductivity Improvement by Iodine Doping for Diamond-Like Carbon Thin-Films Deposited by Microwave Surface Wave Plasma CVD. *Diamond Relat. Mater.* **2006**, *15* (4−8), 645−648.

(13) Adhikary, S.; Tian, X. M.; Adhikari, S.; Omer, A. M. M.; Uchida, H.; Umeno, M. Bonding Defects and Optical Band Gaps of DLC Films Deposited by Microwave Surface-Wave Plasma CVD. *Diamond Relat. Mater.* **2005**, *14* (11−12), 1832−1834.

(14) Choi, J.; Nakao, S.; Kim, J.; Ikeyama, M.; Kato, T. Corrosion Protection of DLC Coatings on Magnesium Alloy. *Diamond Relat. Mater.* **2007**, *16* (4−7), 1361−1364.

(15) Chen, C. W.; Robertson, J. Doping Mechanism in Tetrahedral Amorphous Carbon. *Carbon* **1999**, *37* (5), 839−842.

(16) Compton, R. G.; Foord, J. S.; Marken, F. Electroanalysis at Diamond-Like and Doped-Diamond Electrodes. *Electroanalysis* **2003**, *15* (17), 1349−1363.

(17) Hayashi, Y.; Ishikawa, S.; Soga, T.; Umeno, M.; Jimbo, T. Photovoltaic Characteristics of Boron-Doped Hydrogenated Amorphous Carbon on N−Si Substrate Prepared by R.F. Plasma-Enhanced CVD Using Trimethylboron. *Diamond Relat. Mater.* **2003**, *12* (3−7), 687−690.

(18) Mohamad, R.; Shariff, M. M.; Tetsuo, S.; Takashi, J.; Masayoshi, U. Characterization of Phosphorus-Doped Amorphous Carbon and Construction of n-Carbon/p-Silicon Heterojunction Solar Cells. *Jpn. J. Appl. Phys.* **2003**, *42* (4S), 2339−2344.

(19) Veerasamy, V. S.; Amaratunga, G. A. J.; Davis, C. A.; Timbs, A. E.; Milne, W. I.; Mckenzie, D. R. n-Type Doping of Highly Tetrahedral Diamond-Like Amorphous Carbon. *J. Phys.: Condens. Matter* **1993**, *5* (13), L169−L174.

(20) Zanin, H.; May, P. W.; Fermin, D. J.; Plana, D.; Vieira, S. M. C.; Milne, W. I.; Corat, E. J. Porous Boron-Doped Diamond/Carbon Nanotube Electrodes. *ACS Appl. Mater. Interfaces* **2013**, *6* (2), 990−995.

(21) Hébert, C.; Mazellier, J. P.; Scorsone, E.; Mermoux, M.; Bergonzo, P. Boosting the Electrochemical Properties of Diamond Electrodes Using Carbon Nanotube Scaffolds. *Carbon* **2014**, *71*, 27−33.

(22) Hu, H.; Chen, G.; Zhang, J. Facile Synthesis of CNTs-Doped Diamond-Like Carbon Film by Electrodeposition. *Surf. Coat. Technol.* **2008**, *202* (24), 5943−5946.

(23) Wei, C.; Wang, C.-I.; Tai, F.-C.; Ting, K.; Chang, R.-C. The Effect of CNT Content on the Surface and Mechanical Properties of CNTs Doped Diamond Like Carbon Films. *Diamond Relat. Mater.* **2010**, *19* (5−6), 562−566.

(24) Kinoshita, H.; Ippei, I.; Sakai, H.; Ohmae, N. Synthesis and Mechanical Properties of Carbon Nanotube/Diamond-Like Carbon Composite Films. *Diamond Relat. Mater.* **2007**, *16* (11), 1940−1944.

(25) Wei, C.; Yang, J.-F. A Finite Element Study on the Hardness of Carbon Nanotubes-Doped Diamond-Like Carbon Film. *J. Mater. Res.* **2012**, *27* (01), 330−338.

(26) Zanin, H.; May, P. W.; Hamanaka, M. H. M. O.; Corat, E. J. Field Emission from Hybrid Diamond-Like Carbon and Carbon Nanotube Composite Structures. *ACS Appl. Mater. Interfaces* **2013**, *5* (23), 12238−12243.

(27) Zanin, H.; May, P. W.; Lobo, A. O.; Saito, E.; Machado, J. P. B.; Martins, G.; Trava-Airoldi, V. J.; Corat, E. J. Effect of Multi-Walled Carbon Nanotubes Incorporation on the Structure, Optical and Electrochemical Properties of Diamond-Like Carbon Thin Films. *J. Electrochem. Soc.* **2014**, *161* (5), H290−H295.

(28) Silva, T. A.; Zanin, H.; Saito, E.; Medeiros, R. A.; Vicentini, F. C.; Corat, E. J.; Fatibello-Filho, O. Electrochemical Behaviour of Vertically Aligned Carbon Nanotubes and Graphene Oxide Nanocomposite as Electrode Material. *Electrochim. Acta* **2014**, *119*, 114−119.

(29) Tsukada, J.; Zanin, H.; Barbosa, L. C. A.; Silva, G. A.; Ceragioli, H. J.; Peterlevitz, A. C.; Teofilo, R. F.; Baranauskas, V. Electro-Deposition of Carbon Structures at Mid Voltage and Room Temperature Using Ethanol/Aqueous Solutions. *J. Electrochem. Soc.* **2012**, *159* (3), D159−D161.

(30) Zanin, H. G.; Peterlevitz, A. C.; Teófilo, R. F.; Ceragioli, H. J.; Baranauskas, V. Synthesis and Characterization of Magnetic Nanocrystalline Diamond Films. *Ferroelectrics* **2012**, *436* (1), 96−100.

(31) Zanin, H.; Saito, E.; Marciano, F. R.; Ceragioli, H. J.; Campos Granato, A. E.; Porcionatto, M.; Lobo, A. O. Fast Preparation of Nano-Hydroxyapatite/Superhydrophilic Reduced Graphene Oxide Composites for Bioactive Applications. *J. Mater. Chem. B* **2013**, *1* (38), 4947−4955.

(32) Figueiredo-Filho, L. C. S.; Silva, T. A.; Vicentini, F. C.; Fatibello-Filho, O. Simultaneous Voltammetric Determination of Dopamine and Epinephrine in Human Body Fluid Samples Using a Glassy Carbon Electrode Modified with Nickel Oxide Nanoparticles and Carbon

Nanotubes within a Dihexadecylphosphate Film. *Analyst* **2014**, *139* (11), 2842−2849.
(33) Lourencao, B. C.; Medeiros, R. A.; Rocha-Filho, R. C.; Mazo, L. H.; Fatibello-Filho, O. Simultaneous Voltammetric Determination of Paracetamol and Caffeine in Pharmaceutical Formulations using a Boron-Doped Diamond Electrode. *Talanta* **2009**, *78* (3), 748−752.
(34) Bard, A. J.; Faulkner, L. R. *Electrochemical Methods: Fundamentals and Applications*, 2nd ed.; John Wiley & Sons: New York, 2001; p 833.
(35) Lourencao, B. C.; Silva, T. A.; Fatibello-Filho, O.; Swain, G. M. Voltammetric Studies of Propranolol and Hydrochlorothiazide Oxidation in Standard and Synthetic Biological Fluids Using a Nitrogen-Containing Tetrahedral Amorphous Carbon (ta-C:N) Electrode. *Electrochim. Acta* **2014**, *143*, 398−406.
(36) Vicentini, F. C.; Ravanini, A. E.; Silva, T. A.; Janegitz, B. C.; Zucolotto, V.; Fatibello-Filho, O. A Novel Architecture Based upon Multi-Walled Carbon Nanotubes and Ionic Liquid To Improve the Electroanalytical Detection of Ciprofibrate. *Analyst* **2014**, *139* (16), 3961−3967.
(37) Figueiredo-Filho, L. C. S.; Brownson, D. A. C.; Gomez-Mingot, M.; Iniesta, J.; Fatibello-Filho, O.; Banks, C. E. Exploring the Electrochemical Performance of Graphitic Paste Electrodes: Graphene vs Graphite. *Analyst* **2013**, *138* (21), 6354−6364.
(38) Nicholson, R. S. Theory and Application of Cyclic Voltammetry for Measurement of Electrode Reaction Kinetics. *Anal. Chem.* **1965**, *37* (11), 1351−1355.
(39) Nicholson, R. S.; Shain, I. Theory of Stationary Electrode Polarography. Single Scan and Cyclic Methods Applied to Reversible, Irreversible, and Kinetic Systems. *Anal. Chem.* **1964**, *36* (4), 706−723.
(40) Lavagnini, I.; Antiochia, R.; Magno, F. An Extended Method for the Practical Evaluation of the Standard Rate Constant from Cyclic Voltammetric Data. *Electroanalysis* **2004**, *16* (6), 505−506.
(41) Oliveira, K. M.; Santos, T. C. C.; Dinelli, L. R.; Marinho, J. Z.; Lima, R. C.; Bogado, A. L. Aggregates of Gold Nanoparticles with Complexes Containing Ruthenium as Modifiers in Carbon Paste Electrodes. *Polyhedron* **2013**, *50* (1), 410−417.
(42) Mazloum-Ardakani, M.; Beitollahi, H.; Ganjipour, B.; Naeimi, H.; Nejati, M. Electrochemical and Catalytic Investigations of Dopamine and Uric Acid by Modified Carbon Nanotube Paste Electrode. *Bioelectrochemistry* **2009**, *75* (1), 1−8.
(43) Wang, C.; Li, C.; Wang, F.; Wang, C. Covalent Modification of Glassy Carbon Electrode with L-Cysteine for the Determination of Acetaminophen. *Microchim. Acta* **2006**, *155* (3−4), 365−371.
(44) Li, Q.; Wang, Y.; Luo, G. Voltammetric Separation of Dopamine and Ascorbic Acid with Graphite Electrodes Modified with Ultrafine TiO_2. *Mater. Sci. Eng., C* **2000**, *11* (1), 71−74.
(45) González-Velasco, J. The Linear Sweep Voltametric Method: An Application to the Study of Reversible and Irreversible Processes. *Electroanalysis* **1994**, *6* (9), 711−724.
(46) Thomas, T.; Mascarenhas, R. J.; D' Souza, O. J.; Detriche, S.; Mekhalif, Z.; Martis, P. Pristine Multi-Walled Carbon Nanotubes/SDS Modified Carbon Paste Electrode as an Amperometric Sensor for Epinephrine. *Talanta* **2014**, *125*, 352−360.
(47) Nasirizadeh, N.; Shekari, Z.; Zare, H. R.; Reza Shishehbore, M.; Fakhari, A. R.; Ahmar, H. Electrosynthesis of an Imidazole Derivative and Its Application as a Bifunctional Electrocatalyst for Simultaneous Determination of Ascorbic Acid, Adrenaline, Acetaminophen, and Tryptophan at a Multi-Wall Carbon Nanotubes Modified Electrode Surface. *Biosens. Bioelectron.* **2013**, *41*, 608−614.
(48) Galal, A.; Atta, N. F.; El-Ads, E. H. Probing Cysteine Self-Assembled Monolayers over Gold Nanoparticles—Towards Selective Electrochemical Sensors. *Talanta* **2012**, *93*, 264−273.
(49) Ferreira, M.; Dinelli, L.; Wohnrath, K.; Batista, A. A.; Oliveira, O. N., Jr Langmuir−Blodgett Films from Polyaniline/Ruthenium Complexes as Modified Electrodes for Detection of Dopamine. *Thin Solid Films* **2004**, *446* (2), 301−306.
(50) Harley, C. C.; Rooney, A. D.; Breslin, C. B. The Selective Detection of Dopamine at a Polypyrrole Film Doped with Sulfonated *β*-Cyclodextrins. *Sens. Actuators, B* **2010**, *150* (2), 498−504.
(51) Shankar, S. S.; Swamy, B. E. K.; Mahanthesha, K. R.; Sathisha, T. V.; Vishwanath, C. C. Acetanilide Modified Carbon Paste Electrode for the Electrochemical Detection of Dopamine: A Cyclic Voltammetric Study. *Anal. Bioanal. Electrochem.* **2013**, *5* (1), 19−31.
(52) Wang, L.; Bai, J.; Huang, P.; Wang, H.; Zhang, L.; Zhao, Y. Self-Assembly of Gold Nanoparticles for the Voltammetric Sensing of Epinephrine. *Electrochem. Commun.* **2006**, *8* (6), 1035−1040.
(53) Akyilmaz, E.; Turemis, M.; Yasa, İ. Voltammetric Determination of Epinephrine by White Rot Fungi (*Phanerochaete chrysosporium* ME446) Cells Based Microbial Biosensor. *Biosens. Bioelectron.* **2011**, *26* (5), 2590−2594.
(54) Teixeira, M. F. S.; Marcolino-Junior, L. H.; Fatibello-Filho, O.; Moraes, F. C.; Nunes, R. S. Determination of Analgesics (Dipyrone and Acetaminophen) in Pharmaceutical Preparations by Cyclic Voltammetry at a Copper(II) Hexacyanoferrate(III) Modified Carbon Paste Electrode. *Curr. Anal. Chem.* **2009**, *5* (4), 303−310.
(55) Huang, S.-S.; Tang, H.; Li, B.-F. Electrochemistry of Electropolymerized Tetra(*p*-aminophenyl)porphyrin Nickel Film Electrode and Catalytic Oxidation of Acetaminophen. *Microchim. Acta* **1998**, *128* (1−2), 37−42.
(56) Boopathi, M.; Won, M.-S.; Shim, Y.-B. A Sensor for Acetaminophen in a Blood Medium Using a Cu(II)-Conducting Polymer Complex Modified Electrode. *Anal. Chim. Acta* **2004**, *512* (2), 191−197.